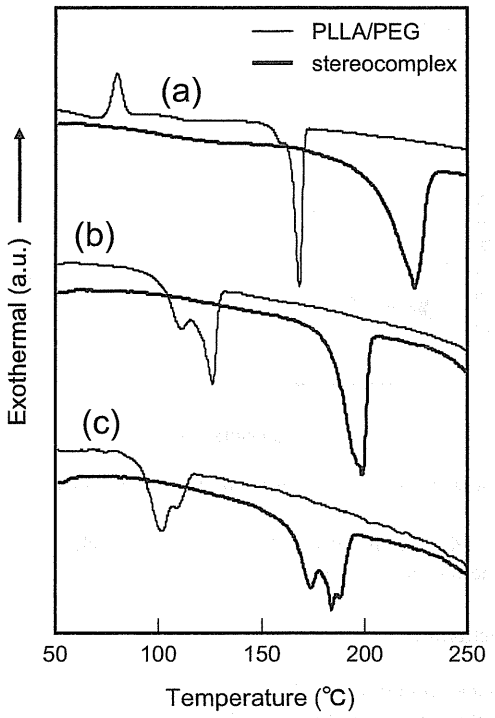

Fig. 2. DSC profiles of the PLLA/PEGs (drawn with lines with normal thickness) and SCs with PDLA (with bold lines): (a) PLLA (run L), (b): run 5, (c): run 6.

polymers contain the unreacted PLLA homopolymers. Copolymer content in the mixture of copolymers and PLLA homopolymers are calculated from the difference between EG content and the estimated one. From runs 1 to 4, the copolymer contents decreased with the decrease in feed PEG ratio because of a low reaction rate with a small amount of reactant. In cases of runs 5 and 6, copolymer contents are high because of a high reaction temperature.

Since PEG is soluble in methanol, low molecular weight block copolymers were removed during the purification process, then most of the observed EG content were smaller than those of theoretical EG content which was calculated from the feed ratio of PLLA and PEG. As for run 6, the EG content is larger than that of theoretical EG content. It is reasonable to say that the removal of lactide took place because of the pyrolysis of PLLA by high reaction temperature.

3.2. Thermal properties

In Table 1, the PLLA used was purchased one and small amount of D-lactide unit was contained. Therefore, T_m was slightly low and ΔH was small compared with those of PDLA which was prepared by the polymerization of D-lactide with high optical purity. The copolymers in runs 3 and 4 showed high ΔHs because of their high LA content. Fig. 2 shows the DSC profiles of PLLA, PLLA/PEGs (runs 5 and 6) and their SCs with PDLA. The melting temperature (T_m) of

Table 2
Thermal properties of SCs of PLLA/PEGs with PDLA.

Run	T_m (°C)	ΔT_m (°C)	ΔH (kJ g^{-1})
L	225	57	63
1	225	61	67
2	223	66	65
3	226	68	54
4	225	64	66
5	199	73	52
6	184	76	33

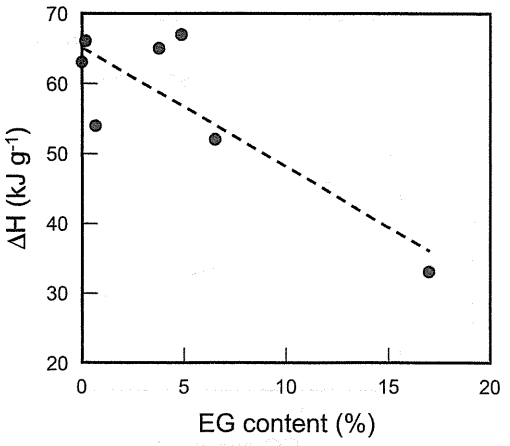

Fig. 3. Enthalpies of fusion of SC vs EG content in PLLA/PEG.

PLLA/PEGs became lower with the decrease in the molecular weight and LA content. In the comparison with runs 5 and 6, the copolymer in run 5 showed higher T_m in spite of the lower molecular weight because of the higher LA content. When PLLA/PEG and PDLA were mixed, the material melted at significantly higher temperatures than each component, suggesting that these two components interact with each other to form SCs. The ΔH values of SCs were always larger than those of the PLLA/PEGs (see Table 2), meaning that the materials became thermally more stable by forming SCs. Fig. 3 shows the relationship between the EG content in PLLA/PEG and ΔH of the SCs with PDLA. It is clearly seen that the value of ΔH decreases with the increase in the EG content. This means that the EG segment suppresses the crystallinity of SC.

When the T_m of the SC is plotted against that of the corresponding PLLA/PEG, a linear relationship was observed with a high correlation coefficient (see Fig. 4). This information enables us to estimate the T_m of the SC from the corresponding PLLA/PEG, and then is useful for the molding process in the polymer industry. The similar tendency was reported for the L-lactide/ε-caprolactone random copolymer and their SCs with PDLA [8].

3.3. Surface hydrophilicity

The surface hydrophilicity of the PLLA/PEGs and their SCs were estimated by measuring the contact angle. As seen in Fig. 5 the

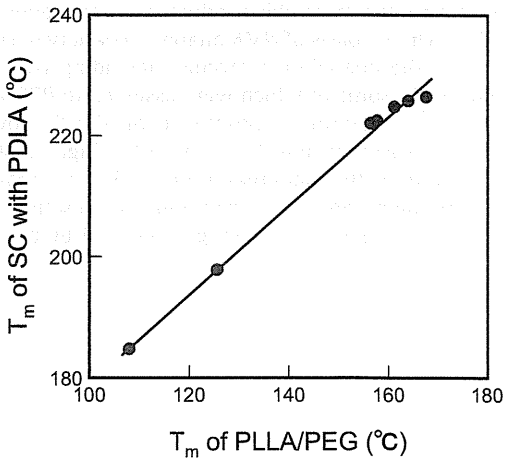

Fig. 4. Relationship between the melting temperatures of the PLLA/PEGs and their SCs with PDLA.

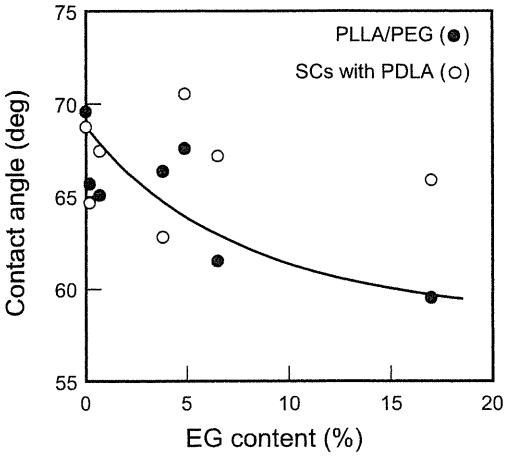

Fig. 5. Contact angle vs EG content of PLLA/PEGs and their SCs with PDLA: (●), PLLA/PEG; (○), SC with PDLA.

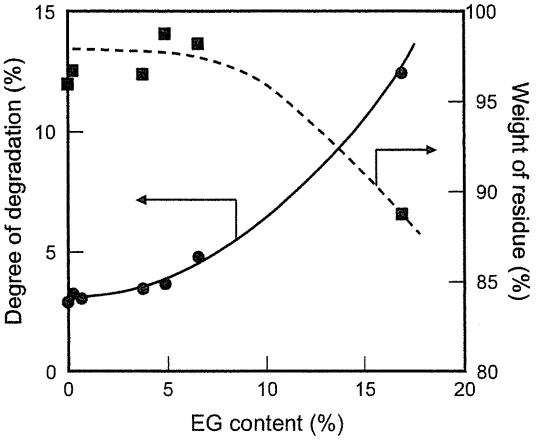

Fig. 6. Biodegradability vs. EG content of the SCs prepared from PLLA/PEG and PDLA.

contact angle significantly decreased with the increase in the EG content of PLLA/PEG (●), showing that the hydrophilicity of PLLA increased by incorporating the EG fragment into the PLLA structure. On the other hand, the contact angle of the SCs with PDLA gave no clear correlation with the PEG content (○). This can be explained that the hydrophilic segment in the structure may be buried or turned into inside when the SC is formed in the chloroform solution, and then the hydrophobic part was arranged outside during the SC formation process, while the detail of the effect of EG fragment on the hydrophilicity is still unclear.

3.4. Biodegradability

PLLA is degradable under the natural environmental conditions, while the SC of PLLA and PDLA is known to have low biodegradability and high hydrolysis-resistance. In order to investigate the contribution of the PEG fragment in the PLLA/PEGs to the degradability, the enzymatic hydrolysis of the SCs of PLLA/PEGs with PDLA was carried out using Proteinase K in the phosphate buffer solution.

Fig. 6 shows the plots of the degradation (left *Y*-axis) and the residual weight (right *Y*-axis) vs. EG content. There are two types of SCs formed with PLLA/PEG and PLLA homopolymers. The SC mixtures seem to be morphologically homogenous because all the data were on the same biodegradation curve. The degradation of the SCs proceeds more with the increase in the EG content of PLLA/PEG, resulting in more water-soluble products and consequently leaving less residues. On the basis of NMR analysis, a variety of compounds was found in the degradation product, including lactic acid and oligo-lactic acids, some of which were assigned to PEG-adducts.

The enzymatic hydrolysis proceeded on the SCs by incorporating the PEG fragment into PLLA. Since the high crystallinity of SCs is thought to be the main reason for the low degradability, the PEG fragment might reduce the crystallinity as described above (cf. Fig. 3). The frayed space or spatial gap induced by the mismatch between PEG fragment and PDLA may give a chance to attack the main chain of lactic acid.

4. Conclusions

A block copolymer of PLLA and PEG was successfully prepared by solvolysis without catalyst. On the basis of the GPC and NMR analyzes the M_n and EG content of the PLLA/PEGs were lower than those expected. The melting temperatures of PLLA/PEGs and their SCs with PDLA showed a linear relationship which enables us to estimate the melting temperature of the SC of PLLA/PEG copolymer and PDLA. The surface hydrophilicity increased with the increase in the EG content of the PLLA/PEGs while no clear dependency of the hydrophilicity on the PEG content was observed in their SCs with PDLA. The incorporating of PEG to PLLA accelerated the enzymatic hydrolysis of the SCs. These findings may lead to the development of a new type of hydrophilic and biodegradable polymer materials based on polylactic acid.

References

[1] Luckachan GE, Pillai CKS. Biodegradable polymers – a review on recent trends and emerging perspectives. J Polym Environ 2011;19(3):637–76.
[2] Ikada Y, Jamshidi K, Tsuji H, Hyon SH. Stereocomplex formation between enantiomeric poly(lactides). Macromolecules 1987;20(4):904–6.
[3] Chang L, Woo EM. A unique meta-form structure in the stereocomplex of poly(D-lactic acid) with low-molecular-weight poly(L-lactic acid). Macromol Chem Phys 2011;212(2):125–33.
[4] Tsuji H, Yamamoto S. Enhanced stereocomplex crystallization of biodegradable enantiomeric poly(lactic acid)s by repeated casting. Macromol Mater Eng 2011;296(7):583–9.
[5] Nouailhas H, Li F, Ghzaoui AE, Li S, Coudane J. Influence of racemization on stereocomplex-induced gelation of water-soluble polylactide–poly(ethylene glycol) block copolymers. Polym Int 2010;59(8):1077–83.
[6] Kakuta M, Hirata M, Kimura Y. Stereoblock polylactides as high-performance bio-based polymers. J Macromol Sci Part C: Polym Rev 2009;49(2):107–40.
[7] Petchsuk A, Nakayama A, Aiba S. Synthesis and biodegradability of L-lactide/glycidol copolymers. Polym Degrad Stab 2009;94(10):1700–6.
[8] Nakayama A, Kawasaki N, Yamamoto N, Aiba S. In: . Proceedings 10th Pacific polymer conference 2007;vol. 6. p. 168.

Biomaterials 34 (2013) 9096–9102

Contents lists available at ScienceDirect

Biomaterials

journal homepage: www.elsevier.com/locate/biomaterials

The effect of electrically charged polyion complex nanoparticle-coated surfaces on adipose-derived stromal progenitor cell behaviour

Ryosuke Iwai [a], Yasushi Nemoto [a,b], Yasuhide Nakayama [a,*]

[a] Division of Medical Engineering and Materials, National Cerebral and Cardiovascular Center Research Institute, 5-7-1 Fujishirodai, Suita, Osaka 565-8565, Japan

[b] Development Department, Chemical Products Division, Bridgestone Co., 1 Kashiocho, Totsuka-ku, Yokohama, Kanagawa 244-8510, Japan

ARTICLE INFO

Article history:
Received 19 July 2013
Accepted 12 August 2013
Available online 2 September 2013

Keywords:
Nanoparticle
Self-organization
Cells
Polyion complexes
Capillary
Aggregate

ABSTRACT

Surface characteristics of biomaterials such as wettability, rigidity, roughness, and electrical charge affect the fate of transplanted cells such as progenitor cells or stem cells for use in regenerative medicine. Of these, the effects of surface electrical charges on cellular behaviour such as adhesion, proliferation, and differentiation are not well understood. We prepared precisely charged culture surfaces ranging from −28 mV to +21 mV, simply by surface deposition of polyion complex nanoparticles prepared by mixing a positively charged thermoresponsive homopolymer, poly(*N,N*-dimethylaminoethyl methacrylate), with negatively charged plasmid DNA at various charge ratios. Drastic morphological changes of adipose-derived vascular progenitor cells were generated on the positively charged surface of organized forms at +19 mV. Capillary-like networks or single aggregates of these cells were selectively created depending on cell seeding density. Our findings offer new insights that may aid develop stem cell-processing techniques for use in regenerative medicine.

1. Introduction

Stem cell research is developing rapidly, and advances in the generation of pluripotent stem cells using embryonic stem cells (ESCs) or induced pluripotent stem cells (iPSCs) as well as the discovery of multipotent adult somatic progenitor cells (SPCs) suggests that the application of stem cell-based therapies in medical fields such as regenerative medicine and drug discovery is highly expected [1–3]. Regenerative medicine is based on tissue engineering technology, in which the transplanted tissues are prepared using three elements: stem cells, biomaterials, which act as cellular scaffolds, and cellular growth factors. One of the most difficult processes in this tissue engineering process is proper control of the proliferation and differentiation of stem cells (ESCs, iPSCs, or SPCs) in order to obtain a sufficient number of functional cells. Maintaining the quality of differentiated transplant cells is also crucial because these cells change or lose their phenotypes depending on the physiological and chemical properties of the biomaterials used in the cell culture substrate [4,5].

It has been recognized that surface characteristics of biomaterials such as rigidity [6,7], wettability (hydrophilicity/hydrophobicity) [8,9], roughness [10,11], electrical charge [12,13], and chemistry [14,15] affect cell functions such as adhesion, proliferation, and differentiation. For example, Yang et al. reported that the rigidity of poly(sodium styrene sulphonate) hydrogel significantly affected the antithrombotic function of human coronary artery endothelial cells following their expression of endothelial cell-specific genes [6]. On the other hand, the influence of surface electrical charge on cellular attachment, proliferation, and differentiation have also been confirmed using surface ionization techniques such as corona discharge treatment or using ionized hydrogels prepared by polymerization of charged monomers [12,13,16]. However, it is difficult to quantitatively vary surface charge densities in such methods without altering other surface properties such as rigidity and chemistry. Therefore, cell behaviour on charged surfaces is inadequately understood at present.

Recently, we developed a bioactive surface having antithrombotic or gene transfectable properties by surface immobilization of antithrombotic heparin or plasmid DNA (pDNA) using poly(*N,N*-dimethylaminoethyl methacrylate) (PDMAEMA), which is a surfactant polymer with both cationic and thermoresponsive characteristics [17,18]. In this surface modification system, the nanoparticles of a polyion complex (PIC) were electrostatically formed by mixing PDMAEMA with negatively charged anionic heparin or pDNA. They get deposited on cell culture surfaces via the hydrophobic interaction between PIC and the culture surface by the

* Corresponding author. Tel.: +81 6 6833 5012x2624; fax: +81 6 6872 8090.
E-mail address: nakayama@ncvc.go.jp (Y. Nakayama).

0142-9612/$ – see front matter © 2013 Elsevier Ltd. All rights reserved.
http://dx.doi.org/10.1016/j.biomaterials.2013.08.027

thermal modulation of hydrophilic/hydrophobic transition of PDMAEMA. Therefore, in our PIC-based surface modification, we could easily modulate surface charge characteristics simply by changing the mixing ratio of PDMAEMA and anionic polymers.

To date, few studies have reported the effects of surface electric charge characteristics on the attachment, growth, and differentiation of ESCs, iPSCs, and SPCs. Therefore, in this study, we prepared surfaces having various charge characteristics with wide range from negative to positive by using PIC nanoparticles of cationic PDMAEMA and anionic pDNA at various mixing ratios. The behaviour of adipose-derived stromal progenitor cells (ADSCs) seeded on these charged surfaces was observed.

2. Materials and methods

2.1. Materials

N,N-Dimethylaminoethyl methacrylate (DMAEMA) was purchased from Wako Pure Chemical Industries (Osaka, Japan). The other chemical reagents were also commercially obtained from Wako. DMAEMA was distilled under reduced pressure before use to remove the stabilizer. The other reagents were purified before use as required.

2.2. General methods

^{1}H NMR spectra were recorded in deuterium oxide (D_2O) using a 300 MHz NMR spectrometer (Gemini 300; Varian, Palo Alto, CA) at room temperature. Gel permeation chromatography (GPC) analyses using *N,N*-dimethylformamide as a solvent were carried out using an HPLC-8320 instrument (Tosoh, Tokyo, Japan) using Tosoh TSKgel SuperAW-4000 and SuperAW-5000 columns. The columns were calibrated with narrow distribution poly(ethylene glycol) standards.

2.3. Synthesis of PDMAEMA

PDMAEMA was synthesized according to the procedure described in our previous report [18]. Briefly, DMAEMA (7.0 g; Tokyo Kasei, Tokyo, Japan) was poured into a glass tube (35 × 65 mm; Maruemu Co., Osaka, Japan) under N_2 gas atmosphere and irradiated for 21 h by using 18-W fluorescent light (FCL20BL; NEC, Tokyo, Japan). After irradiation, re-precipitation was carried out 6 times with chloroform solution in hexane (Kanto Chemical, Tokyo, Japan). The final precipitate was dried under reduced pressure to obtain PDMAEMA (4.3 g, 61.4% conversion). The molecular weight of PDMAEMA was determined to be 9.7×10^4 g mol^{-1} (polydispersity: 4.1) by GPC analysis. ^{1}H NMR: δ 0.8–1.2 ppm (br, $-CH_3$), 1.6–2.0 (br, $-CH_2-CH_3$), 2.2–2.4 (br, $N-CH_3$), 2.5–2.7 (br, CH_2-N), 4.0–4.2 (br, $O-CH_2$).

2.4. Preparation and characterization of PIC

A saline solution (20 μl) of PDMAEMA were dissolved in a DNase-free pure water (Invitrogen, CA, USA) solution (30 μl) of the firefly luciferase-encoding plasmid DNA (pGL3-control vector; Promega, WI, USA) or Cy3-labelled plasmid DNA (*Label* IT® plasmid delivery control-Cy3; Mirus, WI, USA) (concentration: 300 μg/ml) to obtain polymer/DNA ratios from 1 to 16, which corresponded to cation/anion (C/A) ratios. The solutions (total volume, 50 μl) were then mixed using a pipette to generate PIC.

The mean diameters and *z*-potentials of the PIC in a saline solution of the same concentration as that used for cell culture experiments were determined by employing dynamic light scattering (DLS) on Zetasizer Nano S (Sysmex, Kobe, Japan) equipped with a 10-mW He–Ne laser. The data are presented as means ± S.D. ($n = 5$).

2.5. Surface characterization

An aqueous solution of the PIC (50 μl; 160 ng DNA at 20 μg/ml) was diluted with 150 μl of saline, and then added into each well of a 96-well polystyrene (PS) dish (Asahi Glass, Tokyo, Japan). After incubation at 37 °C for 6 h, the culture surfaces were observed by AFM (SPM-9700; Shimadzu, Kyoto, Japan) and fluorescent microscopy, respectively.

The *z*-potential of the PIC-coated PS surface was measured with an ELSZ-1000Z electrophoretic light scattering spectrophotometer (Otsuka Electronics, Osaka, Japan). The PIC having C/A ratio of 1–16 in 580 μl of a saline solution were added to PS culture plates (Asahi Glass) that were cut into 17 mm × 32 mm size and dried at 40 °C for 24 h. After drying, the plates were placed at the bottom of electrophoretic cells filled with distilled water containing surface charge-neutralized PS latex particles, and then, *z*-potential was measured at 37 °C.

2.6. Cell preparation

ADSCs were isolated from rat fat tissue by the method described in our previous study [18]. Briefly, approximately 1 g of fat tissue was obtained from its subcutaneous fatty layer and digested using 0.1% collagenase type I solution (Wako) at 37 °C for 1 h with gentle agitation. After filtering the digest through a 100-μm nylon mesh (BD Biosciences, NJ, USA) and centrifuging it at 1300 rpm for 4 min, the cell pellet was collected. The cell pellet was resuspended in Dulbecco's modified Eagle's medium (DMEM) (Gibco, Invitrogen, Carlsbad, CA) containing 10% foetal bovine serum (Hyclone Laboratories, Logan, UT), penicillin (200 units/ml; ICN Biomedicals, Aurora, OH), and streptomycin (200 mg/ml; ICN) (growth medium; GM). Cell suspensions were then filtered through a 70-μm nylon mesh (BD Biosciences). The cells were placed on a dish (55 cm^2; Asahi Glass) with the growth medium, and cultured in an atmosphere of 5% CO_2 at 37 °C. When the culture was nearly confluent, it was harvested and subcultured at 1.0×10^4 cells/cm^2. The cells were used for experiments before they reached the third passage. Human umbilical vein endothelial cells (HUVECs) were purchased from Lonza (CC-2517; Walkersville, USA), and cultured in endothelial cell basal medium supplemented with 2% FBS and endothelial growth supplements (endothelial medium; EM, CC-3124, Lonza).

2.7. ADSC and HUVEC culture

ADSCs and HUVECs were cultured on the PIC-coated culture surface. Briefly, an aqueous solution of PIC (50 μl; plasmid concentration, 20 μg/ml) having C/A ratios from 1 to 16 was diluted with 150 μl of saline, and then added into each well of 24-multiwell dishes. After incubation at 37 °C for 6 h, the ADSCs and HUVECs ($0.8–3.2 \times 10^5$ cells/well) in 1.0 ml of GM and EM respectively were seeded and cultured in an atmosphere of 5% CO_2 at 37 °C for 2–10 days observed with optical microscope.

2.8. Capillary formation assay

Tube formation assays for ADSCs and HUVEC were performed using Matrigel™ basement membrane matrix (10.2 mg/ml; BD Biosciences) as a positive control. A 24-multiwell dish was coated with 100 μl of Matrigel™ in each well. After incubation at 37 °C for 3 h, ADSCs and HUVECs suspended in GM and EM, respectively, were seeded to each well with 8.0×10^5 cells/well. The culture was incubated in an atmosphere of 5% CO_2 at 37 °C for 2–10 days before being observed with an optical microscope.

2.9. Determination of rat VEGF production

The concentration of rat VEGF in cell culture supernatant was determined by an enzyme-linked immunosorbent assay (ELISA) kit (Quantikine Immunoassay Kits; R&D Systems, Minneapolis, MN). The concentration was expressed as the production of VEGF per 10^5 cells at the time of harvest.

3. Results

3.1. Surface modification by PIC

As demonstrated in our previous study, the diameter of PDMAEMA particles in water was approximately 72 ± 4 nm [18], and it was increased more than two-fold when mixed with a pGL3-control pDNA solution, indicating the formation of PIC of PDMAEMA and pDNA (Fig. 1A). The diameter of the PIC increased with the amounts of PDMAEMA ranging from 116 ± 1 nm to 222 ± 10 nm for C/A ratios of 2 and 16, respectively. On the other hand, a significantly larger particle diameter of the PIC (357 ± 79 nm) was observed at a C/A ratio of 1, in which the number of positive and negative charges were equal.

Although *z*-potential of the PIC had a negative charge of approximately −30 mV at the lowest C/A ratio of 1, it increased drastically and shifted to a positive charge of approximately +19 mV at C/A ratios of 2 (Fig. 1B white symbol). A C/A ratio higher than 2 did not significantly affect *z*-potential value, indicating saturation of positive charges surrounding the PIC particles. The *Z*-potential of PIC-coated PS surfaces increased gradually with C/A ratio from negative (−28 mV) to neutral (±0 mV) and positive charges (+19 mV) for C/A ratios of 1, 2, and 4, respectively (Fig. 1B; black symbol). The positive charge on the surface was saturated at around +20 mV when the PIC having a C/A ratio higher than 4 was coated.

The topography of the PIC-coated PS surface was observed using AFM. At relatively low C/A ratios of 2 and 4, AFM images showed

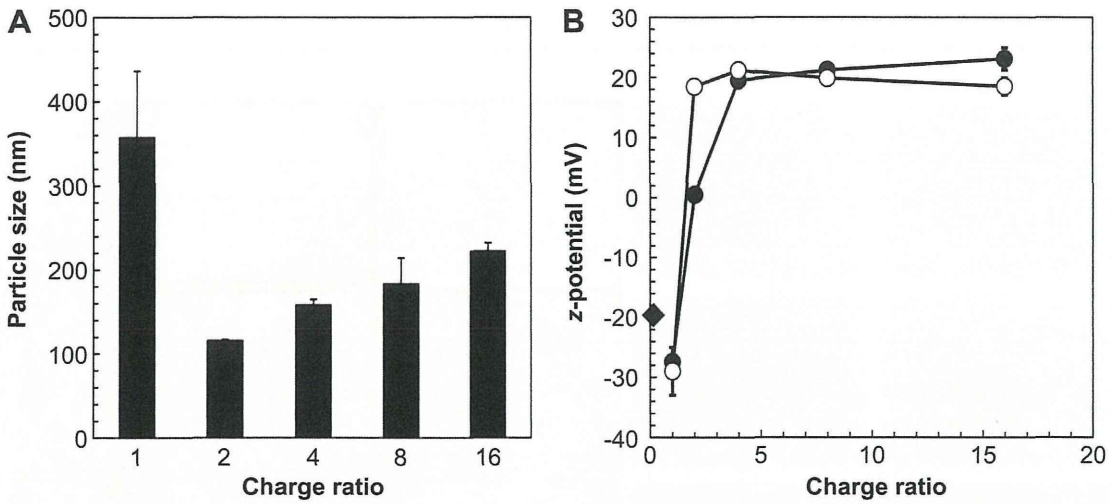

Fig. 1. (A) Particle size of the PIC prepared by mixing PDMAEMA and pGL3-control plasmid DNA with various charges (C/A) ratios ranging from 1 to 16. The values represent the mean ± SD ($n = 5$). (B) The z-potentials of PIC particles (○) and PIC-coated polystyrene (PS) surface (●) with increasing charge (C/A) ratio ranging from 1 to 16. ◆ : z-potential of non-treated PS culture surface. The values represent the mean ± SD ($n = 3$).

rough surface morphology with a number of micron scale particles (Fig. 2A-1, A-2), whereas a striped pattern with an island-shaped large aggregation was observed at relatively high C/A ratios of 8 and 16 (Fig. 2A-3, A-4).

The PIC deposited on the culture surface was visualized by fluorescence microscopy using Cy3-labelled plasmid DNA. Although the red fluorescent particles derived from Cy3-labelled plasmid DNA were clearly observed on the culture surfaces where PICs at C/A ratios of 2 were coated, their fluorescence intensity was decreased with increasing C/A ratio, and little fluorescence was observed at C/A ratio higher than 8, which implies that the fluorescence of Cy3-labelled plasmid DNA was shielded with the excess amount of PDMAEMA (Fig. 2B-1–4). On the other hand, the morphologies of red fluorescent particles observed at C/A ratios 2 and 4 were very similar to those observed in the AFM topography at same C/A ratios.

3.2. Morphological changes in ADSC organization

The adherent shape of ADSCs and HUVECs seeded on the PIC-deposited surface with different C/A ratios of PICs were also observed. Although the ADSCs showed good adhesion with spindle-spread shape regardless of the cell seeding density, the surfaces with PICs having C/A ratios of 1 and 2, had their morphology changed drastically at C/A ratios of 4 and 8, by self organizationally forming cell aggregates and capillary-like networks at day 2 and day 5, respectively, depending on cell seeding density of 4.0×10^4 cells/cm^2 (capillary), 8.0×10^4 cells/cm^2 (capillary or aggregate), and 16×10^4 cells/cm^2 (single aggregate) (Fig. 3A, B). At the highest C/A ratio of 16, ADSCs were dead without adhering to the surface at any cell seeding densities.

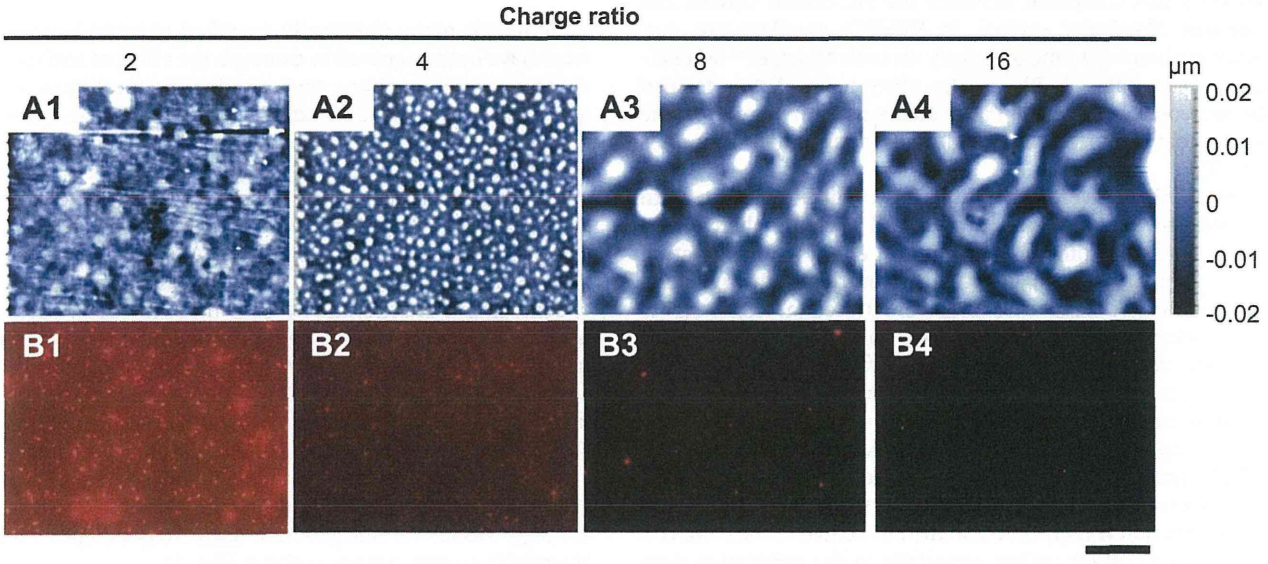

Fig. 2. AFM (A1–A4) and fluorescence microscopy (B1–B4) images of PIC-coated polystyrene (PS) surfaces prepared by using PICs having various charge (C/A) ratios ranging from 2 to 16. Scale bar: 20 μm.

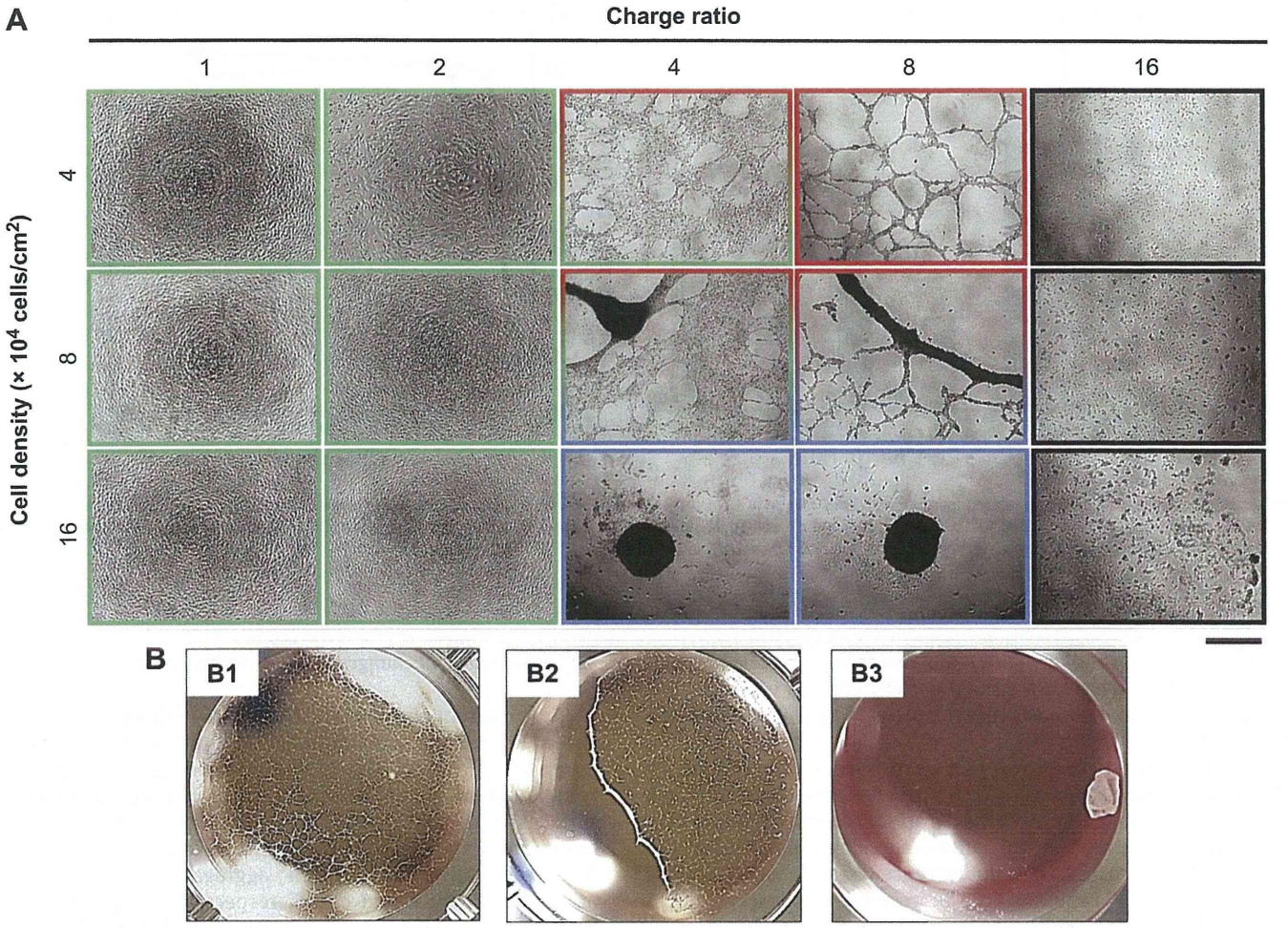

Fig. 3. (A) Phase contrast images of ADSCs cultured on PIC-coated surfaces having various charge (C/A) ratios and different cell seeding densities. Scale bar: 200 μm. (B) Macroscopic images of ADSCs cultured on the PIC-coated 24-multiwell surfaces having a C/A ratio of 8 with different cell seeding densities of 4 (B-1), 8 (B-2) and 16 (B-3) × 10^4 cells/cm^2. Images were captured at 5 days after cell seeding.

The inducibility of capillary-like network formation of ADSCs and HUVECs was compared between the PIC-coated surface and conventional Matrigel™ surface. In HUVECs, capillary-like networks were observed homogeneously on both Matrigel™ and PIC-coated surfaces (Fig. 4A, B). On the other hand, ADSCs formed similar networks only on the PIC-coated surface, whereas on the Matrigel™-coated surface, they formed many small spheroids (Fig. 4C, D).

Although ADSCs were once adhered to culture surface with spindle-shaped shape at day 1 after cell seeding, their shape drastically changed from spindle to round at day 4 of cultivation (Fig. 5A). Capillary tube-like network was then self-organizati onally formed. The capillaries that constituted network structure were elongated and the numbers of their branches were significantly decreased during the cultivation from day 4–8, which indicated maturation of the capillary tubes.

The VEGF production of ADSCs cultured on the PIC-coated surfaces was compared to that of ADSCs cultured on conventional non-treated PS surfaces. VEGF production increased with cultivation time on both surfaces (Fig. 5B). However, a significantly higher rate of VEGF production was observed on the PIC-coated surface than on the non-treated culture surface especially in the cultivation time between day 4 and day 6, consisting with the period that the ADSCs formed capillary tube-like networks.

4. Discussion

Although many chemically modified charged biomaterial surfaces have been prepared to examine the effect of surface electrical charges on cell functions such as adhesion, proliferation, and differentiation in previous studies, most of them were designed to have negatively charged characteristics. Therefore, cell behaviours on positively charged surfaces are poorly understood. In this study, we prepared charged culture surfaces having several electrical charges ranging from negative (−28 mV) to positive (+21 mV) by using the PIC nanoparticles of PDMAEMA and pDNA (Fig. 1B). PDMAEMA is homopolymer having both thermoresponsive and cationic characteristics, and by using these characteristics, we could prepare PICs with various charge ratios by changing the mixing ratio of PDMAEMA and pDNA and deposited PICs on the culture surface only by standing at 37 °C. Therefore, surface precise electrical charges were produced simply by the deposition of PICs.

Because of the cultivation of ADSCs on PIC-coated positively charged culture surface, we could induce the morphological changes of ADSCs with capillary-like networks or single aggregates, although ADSCs cannot generate such morphologies even on the Matrigel™-coated culture surfaces (Fig. 4).

The morphological changes of ADSCs cultured on the PIC-coated surfaces were observed at C/A ratios of the PICs between

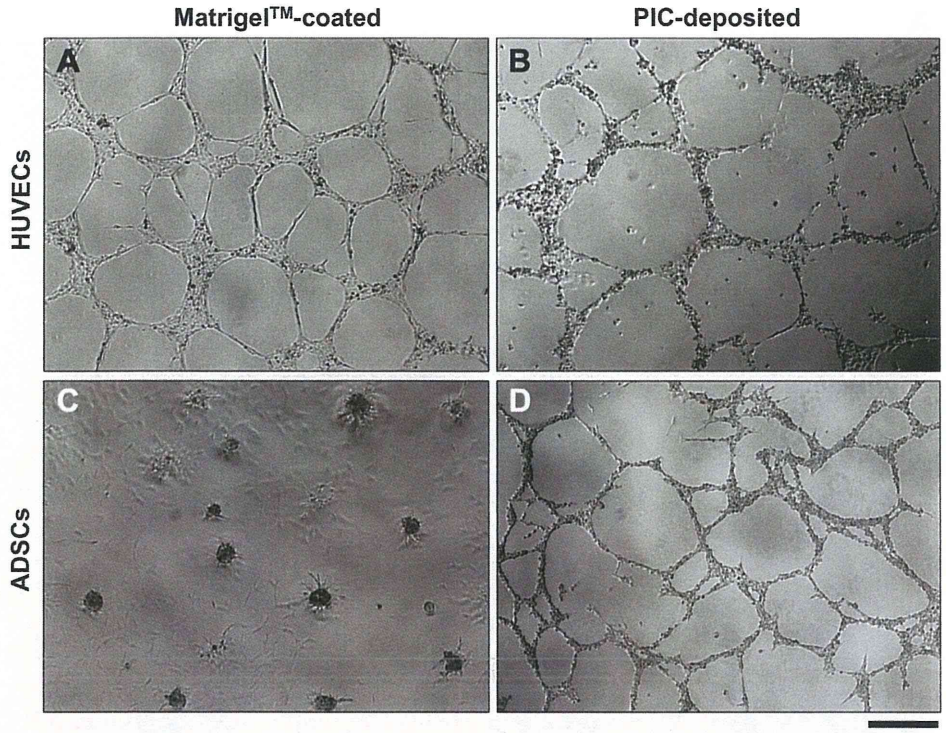

Fig. 4. Phase contrast images of HUVECs (A, B) and ADSCs (C, D) cultured on the Matrigel™-coated (A, C) and PIC-coated (B, D) culture surfaces. The C/A ratio of PICs = 8, cell seeding density = 8.0×10^4 cells/cm^2. Images were captured at 2 days (A, B) and 5 days (C, D) after cell seeding. Scale bar: 200 μm.

approximately 4 and 12, in which the ADSCs formed capillary-like networks or aggregates depending on the cell seeding density (capillary-like networks $< 8.0 \times 10^4$ cells/cm^2 $<$ single aggregates) (Figs. 3 and 6). In general, the shape of adhesive cells is maintained by actin stress fibres, which are known to be linked intimately to integrin families and their related adhesion molecules. Therefore, if the destabilization of integrin-adhesion molecules or adhesion molecules-culture substrates junctions is caused by intra- or extracellular environmental factors, the stress fibres are strained, thereby altering the morphology of the cells [19,20]. Thus, we thought that the aggregate formation observed in this study at very high cell seeding density of 16×10^4 cells/cm^2 occurred because of shrinkage of the confluent ADSCs monolayer. This might be caused by the deformation of actin stress fibres following the destabilization of integrin-adhesion molecules or adhesion molecule-culture junctions triggered by the contact of ADSCs with positively charged culture surfaces. On the other hand, ADSCs did not form single aggregate, but formed capillary-like structure at the cell seeding density of 4.0×10^4 cells/cm [2]. In this relatively low cell seeding density, the cells did not become over-confluent throughout culture and they could spread well without forming tight cell–cell junctions with surrounding cells (Fig. 5A). The cell adhesion was maintained with limited influence of the shrinkage strain of surrounding cells because the cell shrinkage strain could not be transmitted to other cells without forming cell–cell junctions. As a result, both the capillary-like network and single aggregate were observed within the same well when the cells were seeded at the middle density of 8.0×10^4 cells/cm^2 (Fig. 3A, B). Meanwhile, an excess amount of PDMAEMA at C/A ratios higher than 16, led to cell death regardless of the cell seeding density (Fig. 6). Although *z*-potential of PIC-coated culture surface having C/A ratios from 4 to 16 was saturated at approximately +20 mV (Fig. 1B), the outermost layer was gradually covered by the excess amount of PDMAEMA and at C/A ratio of 16, the pDNA was completely coated with the PDMAEMA (Fig. 2B-1–4). Therefore, we considered that the cell death observed at C/A ratio of 16 was caused by the cytotoxicity of PDMAEMA that excessively accumulated on the outermost layer of the PICs.

The electrical charge characteristics of biomaterial surfaces affect not only cellular adhesion and growth, but also cell differentiation state [12,21,22]. For example, Dadsetan et al. reported that the significantly enhanced production of chondrocyte-specific proteins was induced when the chondrocytes were cultured on the negatively charged oligo(poly(ethylene glycol) fumarate) hydrogels [21]. In this study, we observed the self-organized formation of capillary-like structures of ADSCs that were visually very similar to HUVECs on the PIC-deposited positively charged culture surfaces with significantly higher VEGF production than that of ADSCs cultured on conventional PS culture surface (Figs. 4 and 5B). Here, many studies now suggest that VEGF is a crucial factor for both of in vivo angiogenesis and in vitro capillary tube formation of endothelial cells and ADSCs [23–25]. In addition, Lin et al. reported that the ADSCs cultured in gas-plasma treated scaffolds showed significantly higher VEGF production than those cultured on conventional adhesive PS dish with well adhesive spread morphology [26]. Therefore, our overview is that the PIC-coated surface having C/A ratios of 4 and higher decreased the adhesive activity of ADSCs by its positively charged electric character. This unstable adhesion state might have led to enhance VEGF production by ADSCs and as the result, the endothelial lineage cells in ADSCs population formed capillary-like structures in response to this concentrated VEGF. Indeed, ADSCs showed particularly high VEGF production rates between 2 and 6 days after cell seeding which is consistent with the period that ADSCs changed their shape from spread spindle (day 1–2) to round (day 3–4) and completely formed capillary-like networks (day 6) (Fig. 5A, B). However, the detailed molecular mechanism leading to the capillary-like network formation of ADSCs observed in this study is unclear and could be demonstrated in future studies by analysing the molecular signal transduction that might be initiated by the contact of ADSCs with PIC-coated

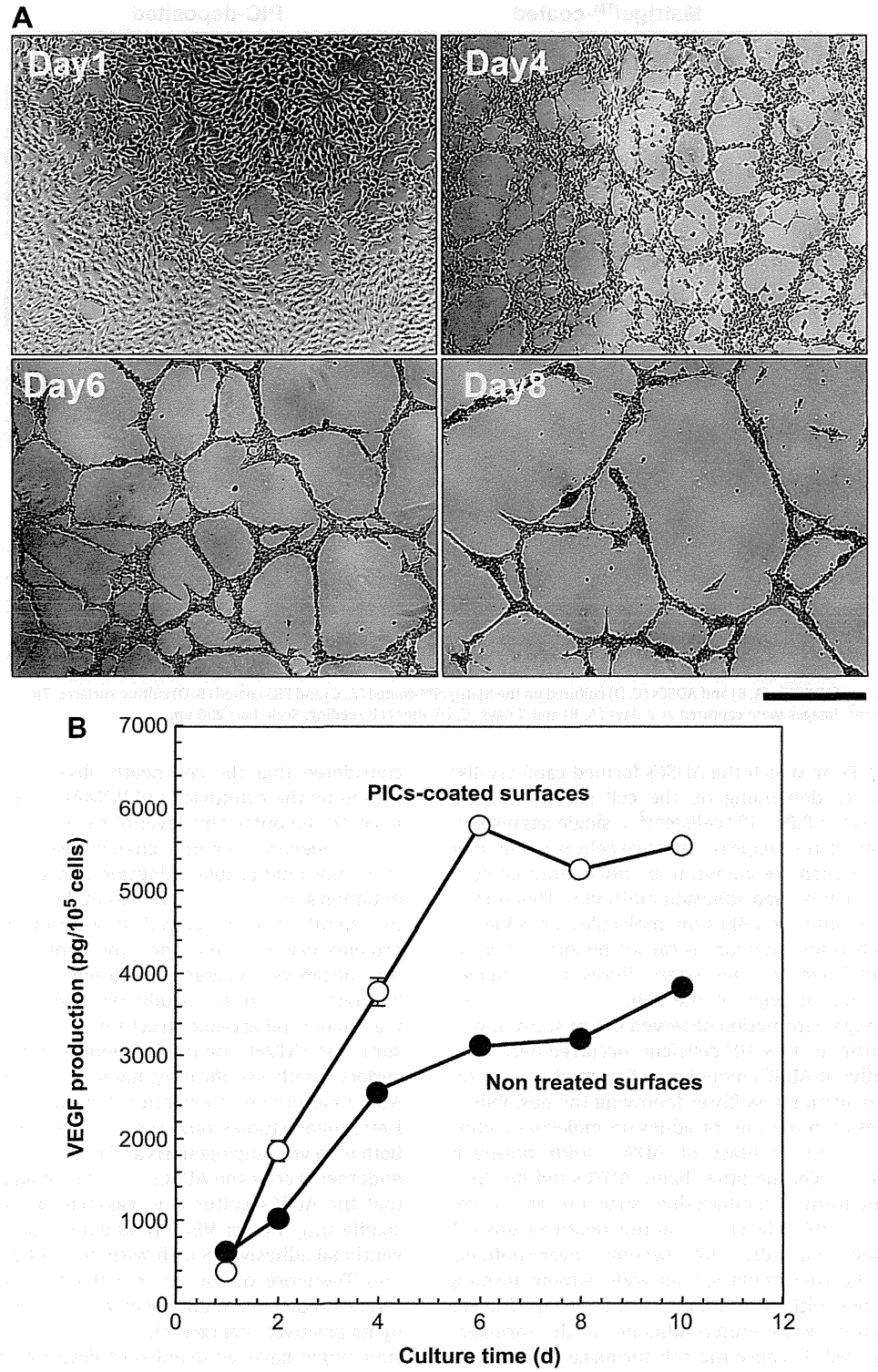

Fig. 5. Morphological changes (A) and rat vascular endothelial cell growth factor (VEGF) production (B) of ADSCs seeded on the PIC-coated culture surfaces (○) and non-treated culture surfaces (●) during the cultivation. The C/A ratio of PICs = 8, cell seeding density = 8.0×10^4 cells/cm^2. Scale bar: 200 μm. The values represent the mean ± SD ($n = 3$).

positively charged surface. In addition to the surface electrical charge, stability to delamination of the deposit PIC layer was considered to cause such morphological changes.

Based on the recent development in cell processing technologies such as cell sheet engineering or 3D cell printing engineering [27,28], many researchers have been endeavouring to prepare thicker engineered tissue transplants that are composed of multiple types of functional cells similar to native organs. To realize this ultimate aim, it is considered necessary to introduce nutrient vessels into transplanted tissues because the central necrosis of transplanted tissues is caused by ischaemia. This vascularization process would require a highly complicated in vitro cultivation system [29]. On the other hand, ADSCs are a heterogeneous cell population, which includes multipotent vascular progenitor cells

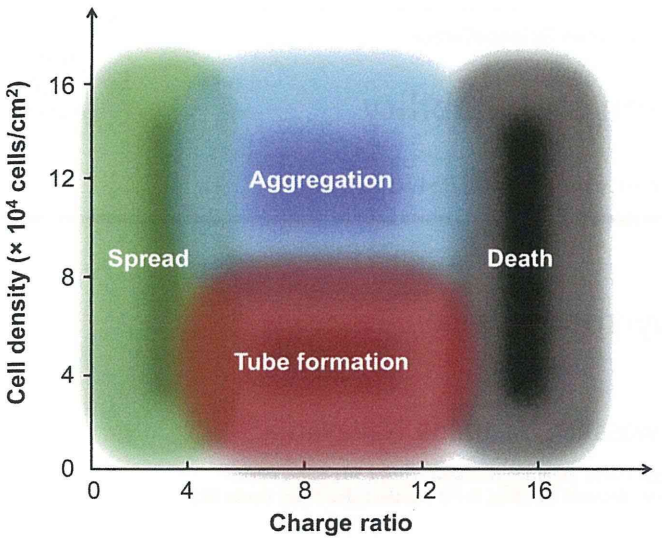

Fig. 6. Effect of the charge (C/A) ratios of PICs and cell seeding density on ADSCs fate.

such as endothelial cells, and smooth muscle cells, and therefore, are known to have angiogenic potential in vivo [30]. However, these ADSCs could not form capillary vessels in any conventional 2D cultivation systems in vitro. In this study, we could successfully induce capillary-like network of ADSCs by seeding them on the PIC-coated positively charged culture surfaces. Therefore, we believe that this capillary vessel like structure of cultured ADSCs would be a useful tool to prepare vascularized thick transplants, which would help in the realization of regenerative medicine.

5. Conclusion

We could prepare precisely charged surfaces with wide ranges from negative (−28 mV) to positive (+21 mV) simply by surface deposition of the ionized PIC that were prepared by mixing PDMAEMA and pDNA with various C/A ratios. The dramatic morphological change of ADSC organization was induced on the positively charged surface, where PICs having C/A ratio of 4 and 8 were deposited. In low-seeding-density homogeneous monolayer of ADSCs was drastically converted to capillary-like network and in high seeding density single aggregate of almost all ADSCs generated. Our findings highlight new insights on the behaviour of stem cells cultured on electrically charged surfaces, which could be useful in the development of cell processing technologies for use in regenerative medicine.

Acknowledgements

This work was supported by grants-in-aid from Ministry of Education, Culture, Sports, Science and Technology and Ministry of Health, Labour and Welfare.

References

[1] Robinton DA, Daley GQ. The promise of induced pluripotent stem cells in research and therapy. Nature 2012;481:295–305.
[2] Bellin M, Marchetto MC, Gage FH, Mummery CL. Induced pluripotent stem cells: the new patient? Nat Rev Mol Cell Biol 2012;13:713–26.
[3] Salem HK, Thiemermann C. Mesenchymal stromal cells: current understanding and clinical status. Stem Cells 2010;28:585–96.
[4] Nikkhah M, Edalat F, Manoucheri S, Khademhosseini A. Engineering microscale topographies to control the cell-substrate interface. Biomaterials 2012;33:5230–46.
[5] Lutolf MP, Gilbert PM, Blau HM. Designing materials to direct stem-cell fate. Nature 2009;462:433–41.
[6] Yang JJ, Chen YM, Kurokawa T, Gong JP, Onodera S, Yasuda K. Gene expression, glycocalyx assay, and surface properties of human endothelial cells cultured on hydrogel matrix with sulfonic moiety: effect of elasticity of hydrogel. J Biomed Mater Res A 2010;95:531–42.
[7] Discher DE, Janmey P, Wang YL. Tissue cells feel and respond to the stiffness of their substrate. Science 2005;310:1139–43.
[8] Wie J, Yoshinari M, Takemoto S, Hattori M, Kawada E, Liu B, et al. Adhesion of mouse fibroblasts on hexamethyldisiloxane surfaces with wide range of wettability. J Biomed Mater Res B Appl Biomater 2007;81:66–75.
[9] Okano T, Yamada N, Okuhara M, Sakai H, Sakurai Y. Mechanism of cell detachment from temperature-modulated, hydrophilic-hydrophobic polymer surfaces. Biomaterials 1995;16:297–303.
[10] Flemming RG, Murphy CJ, Abrams GA, Goodman SL, Nealey PF. Effects of synthetic micro- and nano-structured surfaces on cell behavior. Biomaterials 1999;20:537–88.
[11] Shi X, Wang Y, Li D, Yuan L, Zhou F, Wang Y, et al. Cell adhesion on a POEGMA-modified topographical surface. Langmuir 2012;28:17011–8.
[12] Dadsetan M, Pumberger M, Casper ME, Shogren K, Giuliani M, Ruesink T, et al. The effects of fixed electrical charge on chondrocyte behavior. Acta Biomater 2011;7:2080–90.
[13] Schneider GB, English A, Abraham M, Zaharias R, Stanford C, Keller J. The effect of hydrogel charge density on cell attachment. Biomaterials 2004;25:3023–8.
[14] Han L, Mao Z, Wu J, Zhang Y, Gao C. Influences of surface chemistry and swelling of salt-treated polyelectrolyte multilayers on migration of smooth muscle cells. J R Soc Interface 2012;9:3455–68.
[15] Chua KN, Chai C, Lee PC, Tang YN, Ramakrishna S, Leong KW, et al. Surface-aminated electrospun nanofibers enhance adhesion and expansion of human umbilical cord blood hematopoietic stem/progenitor cells. Biomaterials 2006;27:6043–51.
[16] Rebl H, Finke B, Lange R, Weltmann KD, Nebe JB. Impact of plasma chemistry versus titanium surface topography on osteoblast orientation. Acta Biomater 2012;8:2080–90.
[17] Nakayama Y, Yamaoka S, Nemoto Y, Alexey B, Uchida K. Thermoresponsive heparin bioconjugate as novel aqueous antithrombogenic coating material. Bioconjug Chem 2011;22:193–9.
[18] Iwai R, Kusakabe S, Nemoto Y, Nakayama Y. Deposition gene transfection using bioconjugates of DNA and thermoresponsive cationic homopolymer. Bioconjug Chem 2012;23:751–7.
[19] Mathieu PS, Loboa EG. Cytoskeletal and focal adhesion influences on mesenchymal stem cell shape, mechanical properties, and differentiation down osteogenic, adipogenic, and chondrogenic pathways. Tissue Eng Part B Rev 2012;18:436–44.
[20] Geiger B, Bershadsky A, Pankov R, Yamada KM. Transmembrane crosstalk between the extracellular matrix-cytoskeleton crosstalk. Nat Rev Mol Cell Biol 2001;2:793–805.
[21] Kwon HJ, Yasuda K, Ohmiya Y, Honma K, Chen YM, Gong JP. In vitro differentiation of chondrogenic ATDC5 cells is enhanced by culturing on synthetic hydrogels with various charge densities. Acta Biomater 2010;6:494–501.
[22] Liu JF, Chen YM, Yang JJ, Kurokawa T, Kakugo A, Yamamoto K, et al. Dynamic behavior and spontaneous differentiation of mouse embryoid bodies on hydrogel substrates of different surface charge and chemical structures. Tissue Eng Part A 2011;17:2343–57.
[23] Balwierz AU, Czech A, Polus RK, Filipkowski B, Mioduszewska T, Proszynski P, et al. Human adipose tissue stromal vascular fraction cells differentiate depending on distinct types of media. Cell Prolif 2008;41:441–59.
[24] Carmeliet P. Angiogenesis in health and disease. Nat Med 2003;9:653–60.
[25] Fan W, Sun D, Liu J, Liang D, Wang Y, Narsinh KH, et al. Adipose stromal cells amplify angiogenic signaling via the VEGF/mTOR/Akt pathway in a murine hindlimb ischemia model: a 3D multimodality imaging study. PLoS One 2012;7:e45621.
[26] Lin J, Lindsey ML, Zhu B, Agrawal CM, Bailey SR. Effects of surface-modified scaffolds on the growth and differentiation of mouse adipose-derived stromal cells. J Tissue Eng Regen Med 2007;1:211–7.
[27] Haraguchi Y, Shimizu T, Sasagawa T, Sekine H, Sakaguchi K, Kikuchi T, et al. Fabrication of functional three-dimensional tissues by stacking cell sheets in vitro. Nat Protoc 2012;7:850–8.
[28] Xu T, Zhao W, Zhu JM, Albanna MZ, Yoo JJ, Atala A. Complex heterogeneous tissue constructs containing multiple cell types prepared by inkjet printing technology. Biomaterials 2013;34:130–9.
[29] Asakawa N, Shimizu T, Tsuda Y, Sekiya S, Sasagawa T, Yamato M, et al. Pre-vascularization of in vitro three-dimensional tissues created by cell sheet engineering. Biomaterials 2010;31:3903–9.
[30] Szöke K, Beckstrøm KJ, Brinchmann JE. Human adipose tissue as a source of cells with angiogenic potential. Cell Transplant 2012;21:235–50.

Polymer Degradation and Stability xxx (2013) 1–7

Contents lists available at SciVerse ScienceDirect

Polymer Degradation and Stability

journal homepage: www.elsevier.com/locate/polydegstab

Synthesis and biodegradation of poly(2-pyrrolidone-*co*-ε-caprolactone)s

Atsuyoshi Nakayama [a,*], Naoko Yamano [a], Norioki Kawasaki [a], Yasuhide Nakayama [b]

[a] *Health Research Institute, National Institute of Advanced Industrial Science and Technology, 1-8-31 Midorigaoka, Ikeda, Osaka 563-8577, Japan*
[b] *Division of Medical Engineering and Materials, National Cerebral and Cardiovascular Center Research Institute, 5-7-1 Fujishiro-dai, Suita, Osaka 565-8565, Japan*

ARTICLE INFO

Article history:
Received 13 March 2013
Received in revised form
18 April 2013
Accepted 25 April 2013
Available online xxx

Keywords:
Biodegradable
Biobased
Polyamide 4
Activated sludge
Hydrolysis

ABSTRACT

Copolyesteramides of 2-pyrrolidone with ε-caprolactone were synthesized by ring-opening copolymerization. The copolymers were random-like and their melting temperature and heat of fusion were dependent on the polymer composition. Biodegradation by a polyamide 4 (PA4) degrading microorganism showed rapid degradation in the region of amide-rich polymer composition. On the contrary, enzymatic hydrolysis using a lipase resulted in a different tendency, that is, ester-rich copolymers hydrolyzed rapidly. Activated sludge makes copolymers degrade to CO_2 in wide polymer composition ratio. Copolyesteramides are expected to be applied as an environmentally-friendly plastics or bioabsorbable polymers in medical fields.

1. Introduction

One of the key technologies needed to create a sustainable society is biomass utilization. Typical biobased polymers are poly(L-lactic acid) and bio-polyethylene. Biosynthesis processes of succinic acid and 1,4-butane diol have improved and practical uses of their polymers are considered [1]. However, they are mainly utilized as packaging materials, that is, conventional polymers. Inexpensive polymers based petroleum, like polyolefins are competitors in such a field. Biomass is a resource distributed over the wide area thinly, therefore it is disadvantageous to compete with petroleum-based plastics in cost. On the contrary, engineering plastics are high performance and high-valued polymers. Therefore, high performance biobased polymers have competitiveness. For example, aromatic polymers show strong mechanical properties and high melting temperature. Poly(trimethylene terephthalate) is a famous biobased polyesters commercialized. 1,3-Propane diol can be synthesized from glucose or glycerin [2]. Some PET is produced from bio-ethylene glycol. Polyamides are also important engineering plastics. Several chemical companies have recently introduced a series of biobased polyamides such as PA610, PA1010, PA410 and PA11 [3]. The biomass as the starting material is a recinoleic acid in castor oil, therefore those polymers have a long methylene chain.

The other environmentally-friendly polymers are biodegradable polymers. Huge amounts of polyolefins, polyamides and polyethylene terepthalate are currently used because of their low production cost and stability of properties. These commercial polymers are hardly prone to degrade, and eventually they tend to become environmental pollutants. Biodegradable polymers are expected to act as alternative materials for solving this problem. Several synthetic polymers, such as aliphatic polyesters, copolyesters, and other polymers were reported to be biodegradable by microbes or enzymes [4–11]. Among them, the aliphatic polyesters show excellent biodegradability but their insufficient mechanical properties make them inappropriate for food packaging applications.

Polyamides are superior materials with high strength, a high melting point, but in general, they are not biodegradable. We have reported one of the polyamides, PA4, which can be synthesized from biomass by way of L-glutamic acid, γ-aminobutyric acid and 2-pyrrolidone (PRN) was biodegraded by activated sludge easily [12–14]. PA4 degrading bacterium (*Pseudomonas* sp. ND-11) was isolated

* Corresponding author.
E-mail address: a.nakayama@aist.go.jp (A. Nakayama).

0141-3910/$ – see front matter © 2013 Elsevier Ltd. All rights reserved.
http://dx.doi.org/10.1016/j.polymdegradstab.2013.04.011